Protein Science (2000), *9*:2302–2312. Cambridge University Press. Printed in the USA.

Cysteine-independent polymerization of metallothioneins in solutions and in crystals

TINGJUN HOU,[1,4] YU AN,[2,4] BINGGEN RU,[2] RUCHANG BI,[3] AND XIAOJIE XU[1]

[1]College of Chemistry and Molecular Engineering, Peking University, Beijing 10087, People's Republic of China
[2]College of Life Sciences, Peking University, Beijing 100871, People's Republic of China
[3]Institute of Biophysics, Chinese Academy of Sciences, Beijing 100101, People's Republic of China

(RECEIVED May 2, 2000; FINAL REVISION September 18, 2000; ACCEPTED September 18, 2000)

Abstract

Polymerization of metallothioneins is one of the usually encountered puzzles during the research process of metallothioneins' structure and function. Our work focuses on the cysteine independently occurred polymerization from metallothioneins monomers in different milieus, while it leaves out the aggregation caused by the oxidation of cysteine, because the latter circumstance is the result of purification lapsus. After the purification of metallothioneins monomers, a dynamic light-scattering technique is used to detect the polymerized states of rabbit liver metallothionein I and II in different buffers, which is the first systematical detection of polymerized states of metallothioneins in solutions. The effects of different compositions of each buffer are discussed in details. Steric complementarity, hydrophobic, and electrostatic interaction characteristics are studied, following the modeling of monomers and relevant polymers of rat metallothionein II, rabbit liver metallothionein I and II. These theoretical calculations are the first complete computer simulations on different factors affecting metallothioneins' polymerization. A molecular recognition mechanism of metallothioneins' polymerization in solutions is proposed on the bases of experimental results and theoretical calculations. Preliminary X-ray studies of two crystal forms of rabbit liver metallothionein II are compared with the crystal structure of rat metallothionein II, and the polymerized states in crystal packing are discussed with the knowledge of polymerization of metallothioneins in solutions. The hypothesis, which is consistent with theoretical calculations and experimental results, is expected to construct a connection between the biochemical characteristics and physiological functions of metallothioneins, and this research may give some enlightenment to the topics of protein polymerizations.

Keywords: computer simulations; metallothioneins; molecular recognition; protein polymerization

Metallothioneins (MTs) belong to a special class of proteins that bind unusually large amounts of metal ions. These proteins are ubiquitously distributed in the cytoplasm of animals, plants, and microbes. They are unusually rich in cysteine but contain few aromatic or histidine residues. Their amino acid sequences are highly conserved in evolution. MTs possess two domains of metal-mercapto clusters and have a very special absorption spectrum (Kojima, 1991). The medical significance of MTs is concerned with the delivery and storage of rare elements (Zn^{2+} and Cu^{2+}), resistance to metal and chemical poisons, and protection against alkylating agents, radicals, and radiation. They have important applications in medicine, ecology, and molecular biology (Vallee, 1991).

The crystal structure of a tetragonal form (Melis et al., 1983) of the MT-II crystallized by repetitive seeding technique from rat liver has been reported previously (Robbins et al., 1991). It appears to be the only X-ray structure and the only unabridged structure of any MT deposited in the Brookhaven Protein Data Bank (PDB), but other MT single domain (α- or β-domain) structures have been solved in solution by NMR. We have reported the crystallization of a second MT-II obtained from rabbit liver in a hexagonal crystal form (An et al., 1999). This second MT structure may give further insight into structure–function relationships in MT family of proteins.

During the process of our work of X-ray crystallography on rabbit liver MTs, different polymerized states of MTs are faced. To understand the behavior and mechanism of MTs' polymerization, CA and BA are looked up. To our astonishment, the researches on this topic are very limited (Irons & Smith, 1976; Arthur et al., 1987; Chatterjee & Maiti, 1987; Otsuka et al., 1988; Andersen et al., 1989; Kimura et al., 1991; Palumaa et al., 1992; Palumaa & Vasak, 1992; Gasull et al., 1993; Palumaa & Vaher, 1996; Andersen & Daae, 1998; Hidalgo et al., 1998). Most of the papers concentrate on aggregations caused by oxidation of cystein, which is a problem in purification but seems not to be concerned with physiological functions because only MTs having their normal conformations can have their functions. Even if some useful works

Reprint requests to: Xu X. Jie, College of Chemistry and Molecular Engineering, Peking University, Beijing 10087, People's Republic of China; e-mail: xiaojxu@chemms.chem.pku.cn.
[4]Equivalent authors.

have been done, their classifications of solution buffers are somewhat chaotic. And the technique used to determine the polymerized states of MTs is gel filtration chromatography, which may induce bias in detections. There is a concept about dimerization of MTs that points out that slow concentration-dependent dimerization process is preceded by an initial rapid Cd-induced rearrangement of the monomeric Cd_7–MT structure, and authors have discovered that phosphate anions have specific effects on the polymerization of MTs. In a crystal structure of rat MT-II, Robbins and Stout (1991) give another kind of MT dimers model, in which sodium cations and phosphate anions are involved because these two kinds of ions are necessary in the crystallization of rat MT-II in their experiments.

The research objects of MTs' biochemical characteristics are usually monomers, but MTs' polymers are generally involved in MTs' physiological functions, so researches of these two aspects may not coincide with each other. This paper focuses on the cystein-independent polymerization from MTs monomers in different milieus, while leaves out the aggregation caused by the oxidation cysteine, because the latter circumstance is the result of purification lapsus. Our purpose is trying to discover MTs polymerized states under normal physiological conditions and to construct a connection between the biochemical characteristic and physiological functions of MTs.

Results

Crystallization of rabbit MT-I and -II

Crystals of rabbit MT-I cannot be obtained in all crystallization systems that we have tried. Rabbit MT-II can be crystallized in several systems using sodium sulfate or PEG4K as precipitant (Table 1), the most suitable temperatures are 25 °C for sodium sulfate systems and 20 °C for PEG4K systems.

Preliminary X-ray studies of two crystal forms of rabbit MT-II crystallized from ammonium sulfate are listed in Table 2.

The polymerized states of rabbit MT-I and -II

First, we must declare that the major goal of this paper is to systematically detect the polymerized states of metallothioneins in solutions. We only want to demonstrate that in different solutions the MTs will represent different polymerized states. I believe that it is too difficult for us to perform all experiments in all biological systems. The polymerized states of rabbit MT-I and -II are summarized in Table 3. The reason why these buffers are used is that rabbit MT-II crystals can be obtained from them. pH = 5.6–8.5 and 10.6 is the experimental pH. It should be noticed that in ddH_2O (pH = 7.0) both rabbit MT-I and II exist as monomers, which means that the purified MTs are monomers and there are no aggregations, so the existing behavior of rabbit MTs in other buffers naturally occur, but not systematic error caused by the purity of protein samples.

Table 1. *Crystallization systems of rabbit MT-II*

	Precipitant	
Buffer	$(NH_4)_2SO_4$	PEG 4K
ddH_2O		+
HAc–NaAc (0.1 M, pH 4.6)	+	+
Citrate acid–Na citrate (0.1 M, pH 5.6)	+	+
HCl–Na cacodylate (0.1 M, pH 6.5)	+	+
NaH_2PO_4–Na_2HPO_4 (0.1 M, pH 7.5)		+
Tris–HCl (0.1 M, pH 8.5)	+	+
Tris (25 mM, pH 10.6)	+	+
Tris (12 mM, pH 10.6) & $CaCl_2$ (0.21 M)		+

[a]The buffers in which rabbit MT-II can be crystallized are labeled with "+."

Hydrophobic interactions between monomers in dimers

Table 4 lists the total area, polar area, nonpolar area, and ratio of nonpolar area for these three MT monomers. The difference between total area is slight, but rabbit MT-II has the largest total area and nonpolar area, and its ratio of nonpolar area is larger than the other two MT monomers. Table 5 is the results of total area, polar area, nonpolar area, and observed hydrophobicity for the interfaces of three MT dimers. Similar nonpolar area ratios of monomers and respective dimer interfaces mean no strong hydrophobic interaction between monomers in the dimers. Hydrophobic interactions between proteins are not only determined by the ratio of nonpolar areas, but also determined by the steric complementarity between the hydrophobic surfaces. Figure 1A represents the hydrophobic surfaces of rat MT-II monomer during the formation of dimers. Hydrophobic surfaces between monomers are almost similar between these three MT monomers. After the formation of dimers from monomers, there are several parts of the hydrophobic surfaces that can contact directly and show fairly good steric complementarity, although the hydrophobic areas contacted is not large. Area a in one monomer and area b in another monomer will contact directly, which show certain surface complementarity during the formation of dimers, as shown in Figure 1A. In general, when monomers form dimers, the binding interface is fairly large, and the ratio of hydrophobic residues is a little higher than that of the hydrophilic residues. The hydrophobic residues do not have good contact in the binding interface although some parts of the molecules do. So the hydrophobic interactions between these three MT dimers may not be strong enough to stabilize the dimers.

Hydrophobic interactions between monomers in dimers

In trimer, there is another binding interface between monomer and dimer besides the binding interface between two monomers, which may be important in stabilization of trimer. The binding interface is investigated to study the hydrophobic interactions between the monomer and dimer in the trimer. Each observed hydrophobicity in the trimer interface (Table 6) is much higher than in the respective dimer interface (Table 5). Rat MT-II has the highest observed hydrophobicity in the trimer interface (Table 6). Rabbit MT-II has the largest trimer interface, which is 40% higher than that of the rabbit MT-I and 20% higher than that of the rat MT-II, and has the best steric complementarity, while rabbit MT-I has the worst. So hydrophobic interactions between rabbit MT-I monomers and dimers in trimers are much weaker than those of the other two MTs. These MTs have similar hydrophobic surfaces in the trimer interface. Each hydrophobic complementarity in the timer interface (Fig. 1B) is better than in the respective dimer interface (Fig. 1A).

Table 2. *Crystallization and preliminary X-ray studies of rabbit MT-II*

	Form 1		Form 2	
Protein buffer (P)	Na citrate (0.2 M, pH 5.6)	Tris-HCl (0.2 M, pH 8.5)		Tris solution (1.0 M, pH 10.6)
Protein concentration	5 mg/mL	10 mg/mL		20 mg/mL
Reservoir (R)		$(NH_4)_2SO_4$ (2.4 M, 1.0 mL)		$(NH_4)_2SO_4$ (2.0 M, 1.0 mL)
Hanging drop	P (10 μL) R (5 μL)	P (10 μL) R (10 μL)	P (10 μL) R (5 μL)	P (5 μL) R (5 μL)
Crystal appearing time	1 week	1 week	3 days	2 weeks
Crystallization time	3 weeks	4 weeks	4 weeks	4 weeks
Crystal shape	Hexagonal prism			
Crystal size (mm)	$0.25 \times 0.25 \times 0.10$	$0.30 \times 0.30 \times 0.20$	$0.25 \times 0.25 \times 0.20$	$0.40 \times 0.40 \times 0.30$
Crystal density (g/cm^3)	1.24	1.25	1.24	1.25
Resistance to X-rays	>18 h	>22 h	>18 h	>22 h
Resolution	2.8 Å	2.6 Å	2.8 Å	2.6 Å
Space group	$P6_222$ or $P6_422$		$P6_322$	
Unit cell parameter	a = 113.4 Å b = 113.4 Å c = 219.1 Å	a = 113.4 Å b = 113.4 Å c = 219.6 Å	a = 113.3 Å b = 113.3 Å c = 146.0 Å	a = 113.4 Å b = 113.4 Å c = 146.6 Å
Molecules per asymmetric unit	12		8	
Matthews coefficient	2.49 $Å^3\ Da^{-1}$	2.50 $Å^3\ Da^{-1}$	2.49 $Å^3\ Da^{-1}$	2.50 $Å^3\ Da^{-1}$
Solvent content	57%	57%	57%	58%

Hydrophobic residues in the monomer interface form a continuous hydrophobic core (Fig. 1B). In the dimer interface, Ile49 and Met1 form a hydrophobic area c and d with their neighbor residues, respectively. During trimer formation, areas a and b in the monomer have very good hydrophobic complementarity with areas c and d in the dimer. Higher observed hydrophobicity and better hydrophobic complementarity in each trimer interface than in the respective dimer interface mean hydrophobic interactions between monomers and dimer in the timer are stronger than those between monomers in the dimers.

Comparison of binding interface between monomers in the dimer and binding interface between the monomer and dimer in the trimer shows these two interfaces have distinguished features. The ratio of nonpolar residues area in the trimer interface is greatly higher than that in the dimer interface, and the hydrophobic areas in the trimer interface have better steric complementarity than that in the dimer interface, so hydrophobic interactions in the trimer interface are much stronger than those in the dimer interface.

The electrostatic potentials for conserved residues

Most of the amino acid residues are conserved in the sequences of these metallothioneins. The conserved residues show almost the

Table 3. *The existence behaviors of rabbit MTs in different buffers*

Buffer	MT-I	MT-II
ddH_2O	Monomer	Monomer
HAc–NaAc (0.1 M, pH 4.6)	Dimer	Trimer
Citrate acid–Na citrate (0.1 M, pH 5.6)	Dimer	Trimer
HCl–Na cacodylate (0.1 M, pH 6.5)	Dimer	Trimer
NaH_2PO_4–Na_2HPO_4 (0.1 M, pH 7.5)	Timer and tetramer	Tetramer
Tris–HCl (0.1 M, pH 8.5)	Trimer	Trimer and tetramer
Tris (25 mM, pH 10.6)	Dimer	Dimer and trimer
Tris (12 mM, pH 10.6) and $CaCl_2$ (0.21 M)	Dimer	Dimer

Table 4. *The solvent accessible surface of three monomers*

Name	Total area ($Å^2$)	Polar area ($Å^2$)	Nonpolar area ($Å^2$)	Ratio of nonpolar area (%)
MT-II (rat)	4,842	2,144	2,698	56
MT-I (rabbit)	4,846	2,170	2,681	55
MT-II (rabbit)	4,943	2,099	2,845	58

Table 5. *The observed hydrophobicity of interfaces of three dimers*

Name	Total area (Å^2)	Polar area (Å^2)	Nonpolar area (Å^2)	Observed hydrophobicity (%)
MT-II (rat)	3,271	1,462	1,808	55
MT-I (rabbit)	3,250	1,384	1,867	57
MT-II (rabbit)	3,010	1,351	1,659	55

Table 6. *The observed hydrophobicity of trimer interfaces in three trimers*

Name	Total area (Å^2)	Polar area (Å^2)	Nonpolar area (Å^2)	Observed hydrophobicity (%)
MT-II (rat)	2,441	810	1,631	67
MT-I (rabbit)	2,132	764	1,368	64
MT-II (rabbit)	2,993	1,190	1,803	60

same electrostatic potential distributions, and the differences of the distributions are expressed by the minor nonconserved residues. In these metallothioneins, the 8 Lys and 20 Cys are highly conserved, along with two kinds of metal ions: cadmium and zinc. Figure 2 shows the electrostatic potential surfaces of the conserved residues of rat MT-II, and the other two metallothioneins are generally the same. In Figure 2A, there are five distinguished electrostatic potential areas, including positive ones a, c, and d, and negative ones b and e. In the back of the binding interface, there are four distinguished electrostatic potential areas, including positive ones c and d, and negative ones a and b. Totally, the negative electrostatic potential areas are much larger than the positive ones. When the pH values are 10.6, the formal charges of lysine becomes 0.5|e| from 1.0|e| in the pH 5.6–8.5 range, so the total positive charges of MT monomers reduce 4|e| and the electrostatic potential distributions are much different from those in the pH 5.6–8.5 range. It is naturally deduced that the negative electrostatic potential areas will increase significantly. The binding interface and its back all become more negative (Fig. 2B). The electrostatic potential distributions in the binding interface play an important role during the formation of the dimer from the monomers. When Figure 2A is associated with the model of the MT dimer, area b in one monomer and area d in another monomer (also in part A) will contact directly, thus a relatively large electrostatic attraction will arise. But in the pH 10.6 milieu, the positive electrostatic potential in area d becomes weaker; as a result, the electrostatic attraction becomes weaker.

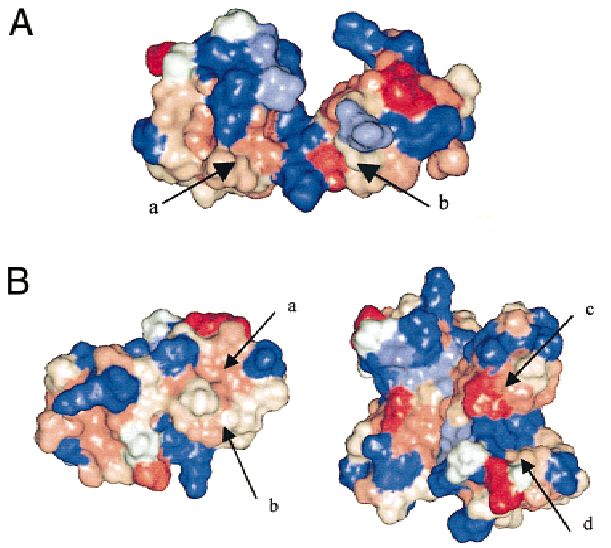

Fig. 1. Hydrophobic surface of (**A**) interface in rat MT-II dimer and (**B**) rat MT-II monomer and dimer in the trimer interface (left, monomer; right, dimer). The monomer on left rotating 180° around the dimer on the right will induce fairly good steric complementarity. In accordance with hydrophobicity of each residue, the solvent accessible suface is mapped with different colors: blue represents the hydrophilic areas, while red represents the hydrophobic areas.

The electrostatic interactions between two monomers in the formation of dimer

Comparison of the electrostatic potential distribution of the conserved residues of these three MTs shows that the negative electrostatic potential areas are larger than the positive ones and distribute more extensively. The electrostatic attractions have contributions to the formation of the dimer. At the same time, the pH value has its effect on the electrostatic potential distributions of the conserved residues. The negative electrostatic areas will become larger in high pH buffers, and the electrostatic attraction becomes weaker.

Besides the effects of the nonconserved residues, they have their particular effects on the electrostatic potential distributions of MT monomers. The factors that should be considered include the conformational change during the formation of the dimer, which can affect the electrostatic potential surfaces also. The electrostatic potential surfaces are studied for these monomers in three MT dimers in different pH buffers. Figure 3 is the electrostatic potential distribution for the rat MT-II in two different pH milieus. The total electrostatic potential distributions are somewhat similar to those of the conserved residues, but there exists a little difference. Compared with the electrostatic potential distributions of the conserved residues, the positive electrostatic potential area become less positive in the binding interface of the dimer significantly. This phenomenon may be caused by the addition of two negative electrostatic residues besides the conserved residues: Asp10 and Glu52. Although these two residues are far away from area a, the long distance electrostatic interaction shows its effect on the electrostatic potential distribution of the whole molecule. Besides area a, both of the negative electrostatic distributions in area b and e become stronger, which also may be the effect of the two residues. When pH value become 10.6, the negative electrostatic potential area becomes larger in the binding interface. In details, the positive electrostatic potential in area a almost disappears, and the positive electrostatic potential in areas c and d become relatively weaker. The electrostatic potential distributions for rabbit MT-I and II in different pH buffers are generally similar to those of rat MT-II. The α-domains are neutral or positive electrostatic potential areas in

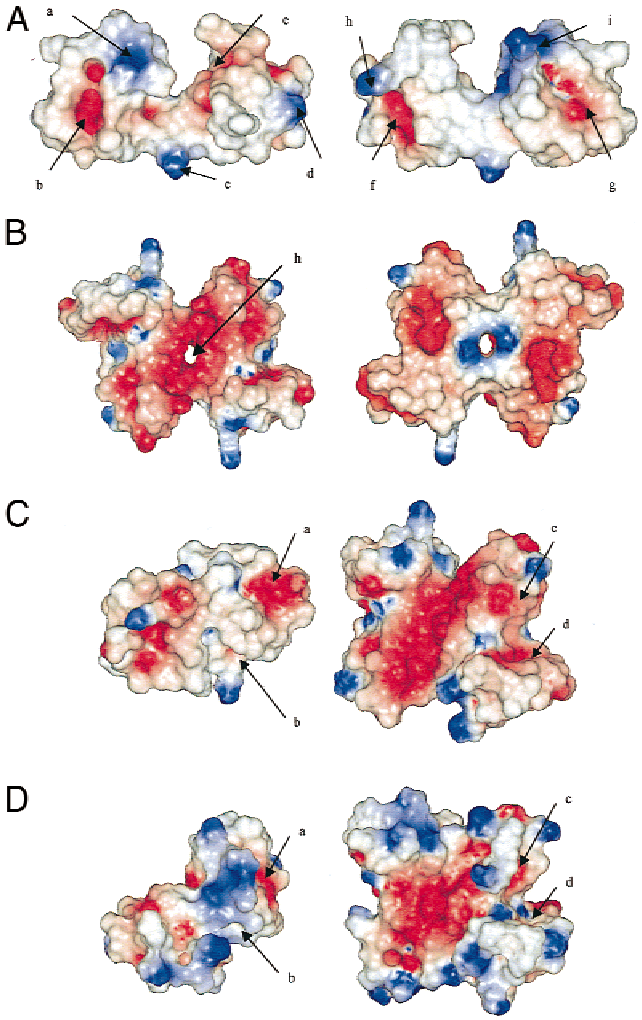

Fig. 2. Electrostatic potentials of (**A**) conserved residues in rat MT-II monomer in pH 5.6–8.5 buffer (left: face to interface, positive areas are a, c, and d, and negative ones b and e; right: back to interface, positive areas are h and i, and negative ones f and g). During the formation of MT dimer, area b and area d in another monomer contact directly, thus relatively strong electrostatic attractions will arise. Electrostatic potentials of (**B**) rat MT-II dimer in pH 5.6–8.5 buffer (the right face is at the rear of the left face) and (**C**) rat MT-II monomer and dimer in pH 5.6–8.5 buffer (left, monomer; right, dimer), and (**D**) rabbit MT-II monomer and dimer in pH 5.6–8.5 buffer (left, monomer; right, dimer).

the binding interface, while β-domains are negative electrostatic potential areas. The α-domain and β-domain in another monomer have electrostatic attraction to some extent, but the attraction is not that strong. When the pH value is higher than the equal point of the side-chain amino of Lys, the electrostatic potential distributions become more negative, and the electrostatic attractions between the two monomers reduce greatly and even show relatively electrostatic repulsions.

Negative electrostatic potential hole

To grasp the electrostatic interactions of the dimers, the electrostatic potential surfaces of the dimers are calculated. Figure 4 is the electrostatic potential surface for the rat MT-II in different pH buffers. It is easy to see that the negative electrostatic potential areas are much larger than the positive ones, and the former ones are concentrated while the latter ones are dispersed. When pH rises to 10.6, whole molecule shows significant negative electrostatic potentials. There is a specific characteristic in binding interface of the dimers: the negative electrostatic potential hole (area h in Fig. 4), which consists of two α-domains of two monomers. In association with Figure 2, area e in the monomer may be important in the formation of the negative electrostatic potential hole.

Because the negative electrostatic repulsion between the two parts of the monomer areas that form it will reduce the stability of the dimers, the negative electrostatic potential hole is unfavorable to the formation of dimers in an energetic respect. The external diameter of the negative electrostatic potential hole is about 5 Å, and its internal may be larger. After the conformational change, it is easy to accommodate some ions or functional groups with a certain size. From an energetic respect, the electrostatic potential distribution of the hole is ready to accept positive charged groups. So the negative electrostatic potential hole is a main accommodation for positive groups, whether in solution or in crystal, and it is big enough to hold several cations—Na^+, Ca^{2+}, etc. The negative electrostatic potential hole may play an important role in stabilizing the dimers. After cations have entered into it, they will have a very strong electrostatic attraction with the negative electrostatic potential areas, which can greatly increase the stability of the dimers. Because the negative electrostatic potential hole is not closed, cations that bind in can move relatively freely, and the exact positions of these cations should not be periodically repeated. Moreover, different kinds of cations have different contributions to the stabilizing effect. In respect to electrostatic interactions, the more positive charges these cations carry, the larger contribution they have in stabilizing the dimers. For instance, Ca^{2+} is more powerful than Na^+ relatively. The negative electrostatic potential hole is also conserved in rabbit MT-I and -II, and the hole is not a closed accommodation for positive groups, and cations bound in can move relatively freely, and the exact positions of these cations should not be periodically repeated.

Electrostatic interactions between monomers and dimers in trimers

Figure 2C shows electrostatic potentials of rat MT-II monomer and dimer in the trimer, and rabbit MT-I has similar electrostatic potentials. In Figure 2C, area a in the monomer and area c in the dimer, and area b in the monomer and area d in the dimer contact directly. Area a in the monomer is mainly negative, area b neutral, area c in the dimer negative with a minor positive region, and area d negative, so electrostatic interactions between the monomer and dimer in the trimer are repulsive. In the pH 10.6 milieu, negative areas increase, and electrostatic repulsions also increase. The trimer is unstable, and even disappears in some buffers.

Rabbit MT-II has more positive electrostatic potentials (Fig. 2D) than rat MT-II and rabbit MT-I. The negative area a in the monomer has positive electrostatic potentials around it, and the negative area c in the dimer become weaker; when they contact, electrostatic repulsions are weak, and even express electrostatic attractions. The weakly positive area b in the monomer contacting with the negative area d in the dimer induce electrostatic attractions. Electrostatic repulsions between the rabbit MT-II monomer and the dimer in the trimer are much weaker than those of the other two

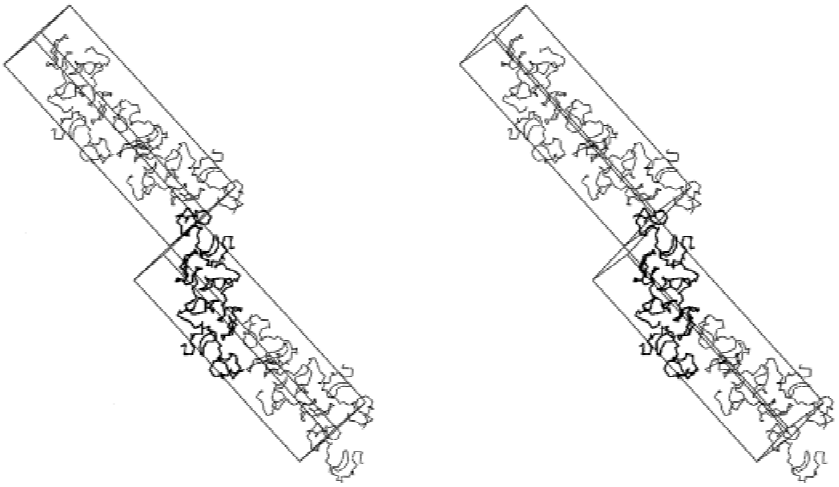

Fig. 3. The crystal packing containing associated tetramer within two neighbor unit cells. (The associated tetramer is shown in a heavy line.)

MTs. With respect to electrostatic interactions, the rabbit MT-II trimer is much more stable than the other two MT trimers, although it is also unstable in pH 10.6 buffers in which area b in the monomer is still positive and the negative electrostatic potential surfaces are smaller than the other two MTs. In comparison with those of the other two MTs, the electrostatic repulsions between rabbit MT-II monomers and dimers in the trimers are much weaker. In respect of the electrostatic interaction, rabbit MT-II trimers are much more stable than the other two MT trimers. In the pH 10.6 buffers, the electrostatic potential surfaces in the binding interface of monomers and dimers will become negative, so the electrostatic interactions will be mainly repulsive. Because area b in the monomer binding interface is still a positive electrostatic potential surface and the negative electrostatic potential surfaces are smaller than the other two MTs, the electrostatic repulsions between rabbit MT-II monomers and dimers in the trimers will be weaker than those of the other two MTs, although the trimers are also unstable when the pH value is over 10.6 because of the electrostatic repulsions between the monomers and dimers. The experimental results show there are rabbit MT-II trimers in the solution, and only rabbit MT-I dimers in the solution. Besides the differences of hydrophobic interactions, the different electrostatic interactions is vital also. When the pH value is about 10.6, the electrostatic repulsions between rabbit MT-II monomers and dimers in the trimers are much weaker than those of rabbit MT-I. In rabbit MT-I trimers, the hydrophobic interactions are not strong enough to overcome the electrostatic repulsions between monomers and dimers, so it is impossible to form stable trimers. According to rat MT-II, the formation of stable trimers is also difficult because of the relatively strong electrostatic repulsions, although the hydrophobic interactions between monomers and dimers in trimers are relatively strong.

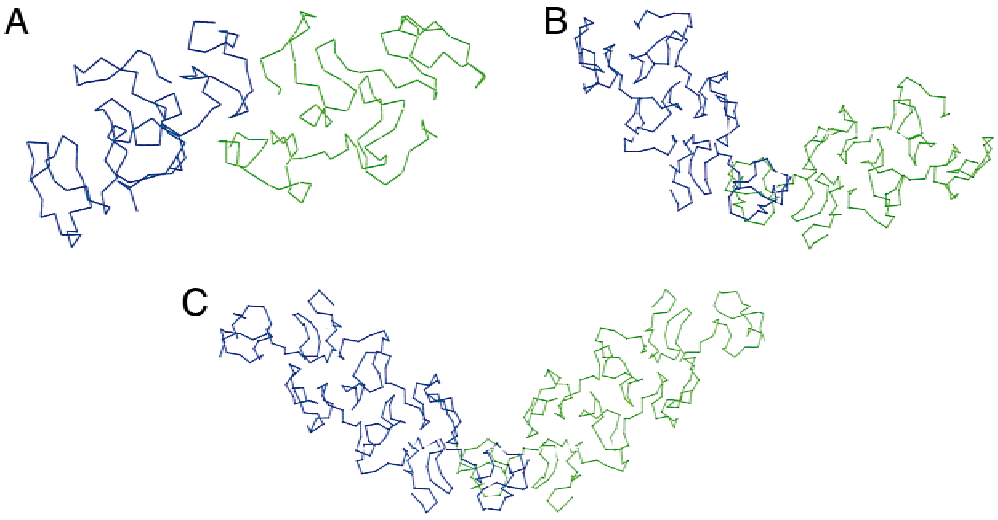

Fig. 4. Interactions between MTs (**A**) dimer and dimer, (**B**) trimer and trimer, or (**C**) tetramer and tetramer in crystals.

Discussion

Effects of crystal systems to polymerization of metallothioneins in solutions

Effects of crystallization systems lie in two ways: first, the composition of crystallization systems specifically bind to proteins molecules and take part in polymerization directly; second, crystallization systems serve as the circumstances for protein polymerization.

1. Sodium cations: Rat MT-II is crystallized from the system: HCOONa as precipitant, NaH_2PO_4–Na_2HPO_4 (pH 7.5) as buffer. In the crystal structure, sodium cations are sited in the negative electrostatic potential cavities formed by the β-domain and α-domain of another monomer in the MT dimer. They are almost closed within the rat MT-II dimer, and periodically repeated along with the protein molecules during crystallization. Sodium cations bound in this way should have their electron densities in a crystal structure. Sodium cations should have bound into the negative electrostatic potential hole formed by the α-domains from the two monomers, which stabilize the conformation of rat MT-II dimers by electrostatic attractions. In summary, sodium cations have their effects on polymerization of MTs in two aspects. The first is binding onto the negative electrostatic potential cavities and partly neutralizing negative electrostatic potential in the binding interface, and the second is binding into the negative electrostatic potential hole and stabilizing the conformation of the MT dimer. Similar electrostatic potentials of these MTs and the conserved negative electrostatic potential hole determine that sodium cations have a similar binding mode and position in these MTs.

2. Ammonium cations: ammonium cations come from precipitant $(NH_4)_2SO_4$ have similar effects of sodium cations.

3. Calcium cations: similarly, calcium cations can stabilize MT dimers like sodium cations, but their higher positive charges induce stronger electrostatic attractions.

4. Phosphate anions: in the crystal structure of rat MT-II, phosphate anions connect Cys19 in the β-domain and Lys31 in the flexible region in the back of the binding interface of the rat MT-II dimer, which restrict the flexibility of the β-domains and keep the trimer interfaces relatively open. The effects of the phosphate anions should be conserved because these amino acids are conserved in these MTs.

Electrostatic interactions are the main effects of metal cations on MTs polymerization. The exchanges between metal cations in MTs and in solutions that have been mentioned in previous research (Melis et al., 1983; Otsuka et al., 1988; Palumaa et al., 1992) seem not to be within the main factors that affect MTs polymerization.

Polymerization of MTs in solutions

Theoretical calculations coinciding with experimental results come from a dynamic light-scattering technique completely. MTs monomers exist only in ddH_2O. In different buffers, MTs exist as dimers, trimers, or tetramers. Polymers beyond tetramers may be caused by oxidation of cysteins, which are not cystein-independent polymerized states of MTs. Certainly, the experimental pHs cannot be simply connected with the physiological functions of MTs, because different kinds of MTs will possess different polymerized states, and different physiological environments will generate different polymerized states. Moreover, until now, the physiological functions of MTs are really not very clear, and relevance of the pHs for physiological functions of MTs are very difficult or impossible for us only from our current materials. MTs' functional conformations are supposed to be different kinds of polymers, i.e., dimers, trimers, or tetramers, and MTs functions are expressed through equilibria between these three kinds of polymers.

1. ddH_2O system: it is expression of MTs themselves and the base to study other solutions and factors. Hydrophobic and electrostatic interactions between MTs monomers cannot stabilize dimer, so MTs exist as monomer. In this system, rat MT-II is supposed to be monomer. Polymerized states in ddH_2O system is an analysis standard of conformational purity of MTs. Other polymers mean aggregation caused by oxidation of Cys has occurred, which is the result of purification lapsus.

2. Acetate–Na acetate, citric acid–Na citrate, and HCl–Na cacodylate systems: these systems belong to one group because pH values belong to the same region: pH 5.6–8.5, sodium cations are common, and anions do not have any particular effects. MTs dimer is stabilized by sodium cations bound in a negative electrostatic potential hole.

   In trimer interface, hydrophobic interactions may not overcome electrostatic repulsions between the rabbit MT-I monomer and dimer, so rabbit MT-I exists as a dimer (Fig. 5A) in solutions.

   Rabbit MT-II has much stronger hydrophobic interactions and weaker electrostatic repulsions than rabbit MT-I between its monomer and dimer, so badly steric complementarity in trimer interface caused by the flexibility of β-domains in the dimer is overcome, and the trimer (Fig. 5B) is formed. After trimer formation, the other trimer interface is almost closed, so the tetramer cannot be formed.

   Rat MT-II has similar electrostatic repulsions and stronger hydrophobic interactions than rabbit MT-I between its monomer and dimer, but hydrophobic interactions may not overcome the combination of electrostatic repulsions and badly steric complementarity caused by the flexibility of β-domains in the dimer, so rat MT-II is supposed to exist as dimers (or with some unstable trimers).

3. Na_2HPO_4–NaH_2PO_4 system: it also has sodium cations and pH value also belong to the pH 5.6–8.5 region, but anions become phosphates that assure fairly good steric complementarity between the monomer and dimer in trimer interface, so rabbit MT-II exists as a tetramer (Fig. 5C). After trimer formation, rabbit MT-I can form only unstable tetramer because of relatively weak hydrophobic interactions in another trimer interface. In this buffer rat MT-II is supposed to exist as tetramer.

4. Tris–HCl system: its pH value also belongs to the pH 5.6–8.5 region, but cations are Tris-H^+, which cannot produce as strong electrostatic attractions as sodium cations. The dimer in which the monomers are not closely bound is favorable to form the trimer. Dimer formation is necessary for trimer formation, and trimer stabilizes the conformation of dimer. So rabbit MT-I exists as a trimer, and rabbit MT-II exists as a trimer and tetramer because of its strong hydrophobic interactions between its monomer and dimer in the trimer interface. Rat MT-II is supposed to exist as a trimer.

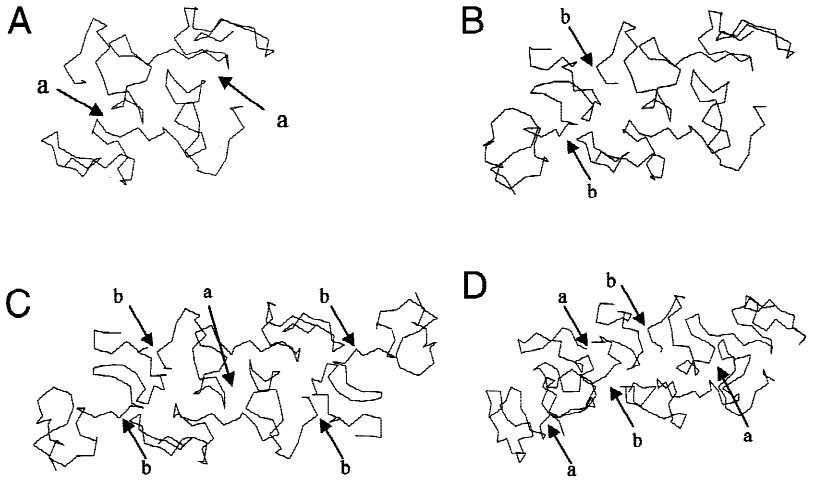

Fig. 5. Construction of MTs polymers. (**A**) dimer, (**B**) trimer, (**C**) tetramer. (1) "a" represents the dimer interface, which is the interface between monomers in a dimer or the interface between monomers in the dimer part in a trimer or tetramer, and "b" represents the trimer interface, which is the interface between a monomer and dimer part in a trimer or tetramer. (2) All models are taken from crystal structure of rat MT-II, and we believe polymerization of MTs in solutions is similar to those in crystals. (3) There are two kinds of tetramers (**C** or **D**) from the crystal structure, but our experiments and calculations show that interactions in the trimer interface are much stronger than interactions in the dimer interface, so only the tetramer shown in **C** is the possible conformation if there are tetramers exist.

5. Tris system: its pH value becomes 10.6, and electrostatic repulsions between the MT's monomer and dimer in the trimer interface increase greatly, so rabbit MT-I exists as a dimer and rabbit MT-II exists as a dimer and unstable trimer. Rat MT-II is supposed to exist as a dimer.

   After the addition of $CaCl_2$, stronger electrostatic attractions of Ca^{2+} than Na^+ bound in a negative electrostatic potential hole result in more closely bound MTs dimers, so rabbit MT-I and II exist as a dimer, and rat MT-II is supposed to exist as a dimer also.

Crystallization and crystal growth of MTs

Rabbit MT-I cannot crystallize in any system that we have tried, while rabbit MT-II crystallize in many systems, and rat MT-II crystallize in a specific system.

These MTs have good steric complementarity. Interactions between two monomers in the MTs dimers are similar, but interactions between MTs monomers and dimers in the trimer interfaces are different from each other. In the trimer interfaces, rabbit MT-I and rat MT-II have similar electrostatic repulsions, while rabbit MT-II has much weaker repulsions or even has slight electrostatic attractions; in respect of hydrophobic interactions, rabbit MT-I is the weakest, rat MT-II the middle, and rabbit MT-II the strongest. Interactions of rat MT-II monomer and dimer in the trimer interface seem to be within a critical value region, which overcome the badly steric complementarity caused by the flexibility of β-domains in the dimer to form a tetramer only with the help of phosphate anions, so rat MT-II crystallizes only in a specific system. Interactions of the rabbit MT-I in the trimer interface seem to be under the critical value region, so this MT cannot crystallize even in a phosphate buffer. Rabbit MT-II has stronger interactions than the critical value region in the trimer interface, so it crystallizes in different crystallization systems.

Interactions in the trimer interface seem to be more important than interactions in dimer interfaces on MT's crystallization ability. First, MTs cannot crystallize unless interactions in the trimer interface are beyond a critical value. Second, crystallizations of MTs become easier, and systems in which MTs can crystallize become more if interactions in the trimer interface become stronger. To obtain MT's crystal, the strategy should be to increase interactions in the trimer interface.

Should rat MT-II crystallize from dimers or tetramers?

Rat MT-II crystals are tetragonal, space group $P4_32_12$, $a = b = 30.9$ Å, $c = 120.4$ Å, and one molecule per asymmetric unit. Robbins and Stout (1991) believe that rat MT-II exists as a dimer in solution, and the crystallization may proceed from dimers rather than monomers. Their reasons lie in two aspects. First, the crystal packing contains intimately associated pairs of molecules related by the twofold axes. Second, a cation of crystallization is trapped between the twofold-related MT molecules. Intuitively, a dimer would crystallize more readily than a monomer because motion of the α- and β-domains about the linker could be restricted by head-to-tail packing of α/β' and β/α'. The dimer model partly explains effects of sodium cations and phosphate anions.

The dimer model explains only one of the effects of sodium cations and only one of the effects of phosphate anions, but sodium cations and phosphate anions have more important functions that we have described above in details. Dynamic light-scattering results show rabbit MT-II exists as a tetramer and rabbit MT-I as a trimer and unstable a tetramer in sodium-phosphate buffer. According to our theoretical calculations of electrostatic and hydrophobic interactions, rat MT-II should have stronger interactions in the trimer interface than those of rabbit MT-I, so rat MT-II should exist as a tetramer in phosphate and sodium solution rather than a dimer. In our opinion, conformational units in solution and crystals should be the same during crystallization equilibrium, and studies of these two aspects can give unification of polymerized states in solutions and crystals, which can clarify some misunderstanding concepts in each field and may give further insight into the nature

of metallothioneins' polymerization. That is to say, the crystallization of rat MT-II should proceed from a tetramer rather than a dimer. In the crystallization system of rat MT-II, the hanging drop is consisted of sodium formate and potassium phosphate, and the reservoir is sodium formate of higher concentration. With sodium cations and phosphate anions, rat MT-II should exist as a tetramer. During the procedure of crystallization, the concentration of sodium cations increase, which is favorable to the packing of tetramers through the interactions of monomers in a dimer interface. And finally, we found out that the crystal packing contains associated tetramers within two neighbor unit cells (shown in heavy lines in Fig. 3). The interactions between two tetramers are shown in Figure 4, which is the same as the those of dimer in the dimer interface.

Polymerization of rabbit MT-II in crystals

The crystallization of rabbit MT-II may proceed from the tetramer, the trimer, the dimer, and the monomer, because its interactions in the trimer interface are different from those of rat MT-II.

1. Tetramer model: in the sodium-phosphate system, rabbit MT-II and rat MT-II have similar polymerized states.
2. Trimer model: in acetate acid–Na acetate, citric acid–Na citrate, and HCl–Na cacodylate buffers, the crystallization proceeds from trimers, because interactions in the trimer interfaces overcome the badly steric complementarity to form stable trimers, and the other trimer interface is almost closed. Interactions between two trimers are similar to but not the same as those in dimer (Fig. 4B).
3. Dimer model: in Tris solution, rabbit MT-II exists as dimers and unstable trimers. After addition of $(NH_4)_2SO_4$, ammonium cations stabilize the conformation of dimers and the equilibrium changes toward dimers; thus, the crystallization proceeds from the dimers. Interactions between the MT dimers are similar to but weaker than those between the monomer and dimer in the trimer (Fig. 4A).
4. $(NH_4)_2SO_4$–Tris–HCl system: in the Tris–HCl buffer, rabbit MT-II exist as trimers and tetramers. After $(NH_4)_2SO_4$ being added, ammonium cations stabilize the conformation of their dimer parts. Tetramers depolymerize, and dimers and trimers are left in solution. If crystal appearing time is 3 days, dimers have not changed to trimers, and the crystallization initiates from dimers; if the time is 1 week, dimers have changed to trimers, then the crystallization proceeds from the trimers. Crystals proceeded from the dimers should be dynamics products; crystals proceeded from the trimers thermodynamics products.
5. Monomer model: in ddH_2O, rabbit MT-II exists as monomers. Addition of PEG4K enhances electrostatic attractions between MT monomers and crystallization becomes possible. Interactions of crystal packing are weak, and crystals mainly grow in two dimensions.

Regulation of MTs crystal forms

Similar steric complementarities determine that crystal packing positions of different kinds of MTs are similar. Crystal packing of MTs is refined by interactions in dimer interface and trimer interface. In rat MT-II, the ratio of interactions between the dimer interface and trimer interface is within a critical value region, in which all dimer interface and trimer interfaces are completely used, and the steric complementarity of MTs is fully satisfied, so the crystallization proceeds from the tetramers.

If interactions in the dimer interface increase or interactions in the trimer interface decrease, one trimer interfaces is almost closed and only one trimer interface's steric complementarity is satisfied, so crystallization may proceed from the trimer. If interactions in the dimer interface become stronger or interactions in the trimer interface become weaker, both trimer interfaces are partly closed, but the extent of closing is weaker than only one trimer interface being closed, so relatively weak interactions exist in both trimer interfaces in crystals. The crystallization initiates from the dimer. If interactions in the dimer interface decrease or interactions in the trimer interface increase, the crystallization proceeds from the monomer.

Material and methods

Protein induction and purification

A rabbit (specie, *Chinchilla giganta*; sex, male; body weight, 2.5–3.5 kg) is subcutaneously injected six times with $CdCl_2$: 1 mg Cd/kg body weight on the first and third day; 2 mg Cd/kg body weight on the fifth and seventh day; 4 mg/kg body weight on the 10th and 12th day. On the 14th day, the rabbit is sacrificed, and its liver immediately removed. The liver is cut into small pieces and homogenized in a precooled solution of 0.01 M Tris–HCl buffer (pH 8.6), ethanol, and chloroform (1.00:1.03:0.08 by volume). Three volumes of the above solution are added, followed by centrifuging at 15,000 × *g* at 277 K for 20 min. The supernatant liquid is maintained at 353 K for 5 min, cooled in ice, and centrifuged at 10,000 × *g* at 277 K for 30 min. Three volumes of precooled ethanol (253 K) are subsequently added to the supernatant. The solution is allowed to stand at 253 K overnight. The precipitate is collected by centrifugation at 277 K for 20 min and dissolved in 0.01 M Tris–HCl buffer (pH 8.6):0.25 mL/g wet tissue, centrifuged at 8,000 × *g* at 277 K for 10 min. The supernatant is loaded on to a Sephadex G-50 column, and eluted with 0.01 M Tris–HCl buffer (pH 8.6). The fractions containing MT are collected and applied to a DEAE Sepharose Fast Flow column and pre-equilibrated with 0.01 M Tris–HCl buffer (pH 8.6). Elution is carried out by salt solution of linear gradients (A buffer:0.01 M Tris–HCl buffer, pH 8.6; B buffer:0.25 M Tris–HCl buffer, pH 8.6). MT-I and MT-II are collected, respectively, and concentrated to suitable volume by lyophilization, then applied to a Sephacryl S-100 column equilibrated with 0.01 M ammonium carbonate for desalination. MT-I and MT-II, 6.8 kDa, are finally lyophilized and stored at 253 K separately.

Mass spectroscopy results show no polymer peaks. The amount of metals in both rabbit MT-I and -II are detected to be 5 Cd/MT and 2 Zn/MT by atomic absorption spectroscopy on PU9200 spectrometer (Philips, Inc., Cambridge, UK). The amino acid sequences of rabbit MT-I and -II are determined on Model 491A sequencer (Applied Biosystems, Inc., Foster City, California) as follows (Fig. 6).

Crystallization and preliminary X-ray studies of rabbit MT-II

Crystallization trials are carried out by the hanging drop vapor diffusion method at 4, 20–28, and 37 °C. The crystal density is

```
                    0         10        20        30
MT-I (rabbit)   :   MDPNCSCATGNSCTCASSCKCKECKCTSCK
MT-II (rabbit)  :   MDPNCSCATRDSCACASSCKCKECKCTSCK
                         40        50        60
MT-I (rabbit )  :   KSCCSCCPAGCTKCAQGCICKGASDKCSCCA
MT-II (rabbit)  :   KSCCSCCPAGCTKCAQGCICKGALDKCSCCA
```

Fig. 6. Amino acid sequences of rabbit MT-I and -II.

measured with pyridine and chloroform mixture linear density gradient or Ficoll density gradient. X-ray diffraction data are collected using oscillation method (oscillation angles 1°) with a Rigaku R-AXIS II imaging plate detector (Rigaku, Inc., Tokyo, Japan) or Mar Research imaging plate detector (Mar Research, Inc., Hamburg, Germany) mounted on a Riguku RU-200 rotating anode X-ray generator (Rigaku, Inc.) operated at 50 kV, 100 mA, with Cu Kα radiation filtered by a graphite monochromator. The data are indexed, integrated, and reduced on a SGI workstation using R-AXIS software or Mar Research HKL and Mar-DENZO provided with the instruments.

Rabbit MT-I cannot be crystallized in any system that we have tried. Rabbit MT-II is crystallized using $(NH_4)_2SO_4$ (25 °C)and PEG4K (20 °C) as pecipitant (Table 1), and preliminary X-ray studies of two crystal forms from $(NH_4)_2SO_4$ are listed in Table 2.

Dynamic light scattering

Polymerized states of rabbit MT-I and -II in different buffers are detected by the DynaPro-801 (Protein Solutions, Inc.). The DynaPro-801 is highly sensitive to trace amounts of aggregation and would otherwise go undetected using other typical characterization techniques. Concentration of rabbit MTs is determined to be 8 mg/mL by referring to concentration sensitivity curve of DynaPro-801. All samples are filtered using Whatman Anotop™ Plus syringe filters of 0.1 m porosity while injecting samples with 0.02 μm filters. The 250 μL syringe is filled with sample. Any trapped air bubbles are removed by tapping gently outside of the syringe with the needle pointing upward. After sample injection, monitor the photon count rate via Dynamics software. The photon count rate should settle to point where it varies not more than 5%. A sample (certain concentration of rabbit MT-I or II in certain buffer) is measured three times, and each time 10–15 measurements are taken before stopping, to ensure that the data are consistent and accurate. The measurements and calculations reported are: measurement time, scattering amplitude, translational diffusion coefficient (D_T), hydrodynamic radius (R_H), estimated molecular weight (MW), polydispersity value, temperature of the sample cell, photon count rate, baseline, and sum of squares (SOS). The estimated molecular weight is calculated from the hydrodynamic radius using an empirically derived relationship between hydrodynamic radius (R_H) and molecular weight (MW) parameters for a number of well-characterized globular proteins in buffered aqueous solutions.

The polymerized states of rabbit MT-I and -II are summarized in Table 3. These buffers are used because rabbit MT-II can be crystallized from them. Rabbit MT-I and -II exist as monomers in ddH_2O, which means the existing behaviors of rabbit MTs in other buffers are naturally occurred, but not systematic error caused by purity of protein samples.

Building the models of dimers and trimers

The crystal structure of rat MT-II is used as a reference protein to get the monomer models of rabbit MT-I and -II by homology modeling (sequence homology is 0.84 and 0.83, respectively) using Homology module in InsightII (Molecular Simulation, Inc., Burlington, Massachusetts).

The unit cell of rat MT-II is modeled using the Crystal module in Sybyl6.5 (Tripos, Inc., St. Louis, Missouri), and its dimer model is the molecules connected by symmetry operators 1 and 6. Another molecule connected by symmetry operator 3 in the same unit cell also has intermolecular contacts with the dimer, so these three molecules are used as the model of a trimer. The dimer and trimer models of rabbit MT-I and II are created from respective models of rat MT-II using superposition operation in InsightII.

All three dimers and trimers are refined using molecular mechanism and dynamics with ESFF (Extensible Systematic Force Field) force field (S.G. Shi, unpublished force field). Energy minimizations are accomplished by 500 cycles of steepest descent algorithms followed by conjugated gradient minimizations until each maximum derivative is within 0.5 kcal/Å/mol. A 15 Å thick water shell is generated to solvate the dimers and trimers. During subsequent molecular dynamics and minimizations, the water molecules in the inner 8 Å thick shell are tethered with a force constant of 50 kcal/Å/mol, while oxygens in the outer shell are fixed; this prevented water molecules from "boiling off." Then, molecular dynamics is carried out at 300 K for about 20 ps. Finally, the dimers and trimers are re-minimized using a 0.2 kcal/Å/mol convergence criterion for the maximum derivative.

The characteristics of hydrophobicity

Solvent-accessible surface area (ASA) is following the definition of Lee and Richards (1971), with a probe radius of 1.4 Å. For monomers, a residue X is classified as a surface one if its ASA is above 20% of the ASA calculated for the extended tripeptide Gly-X-Gly. Otherwise, it is classified as an interior residue. The procedure of Tsai et al. (1997) is adopted to determine the interior interface residue. For a dimer or trimer, its ASA is calculated twice: once for the complex, and the other for uncomplexed subunits composing the dimer or trimer. If the ASA difference is greater than 10%, the residue is classified as buried in the interface.

The quantity based on ASA is used to measure the hydrophobic effect at the interface:

$$\frac{{}^{Non}\mathrm{ASA}^I + {}^{Non}\mathrm{ASA}^J}{{}^{Non}\mathrm{ASA}^I + {}^{Pol}\mathrm{ASA}^J + {}^{Non}\mathrm{ASA}^I + {}^{Pol}\mathrm{ASA}^I} \qquad (1)$$

where ^{Non}ASA and ^{Pol}ASA are the nonpolar and polar surface areas that are buried by partner subunits.

The Connolly surfaces of these MTs are calculated and displayed using InsightII. The solvent accessible surface is mapped with different colors—blue representing hydrophilic areas, red hydrophobic areas.

Calculation of electrostatic potentials

Electrostatic potentials of rat MT-II, rabbit MT-I and -II are calculated by the finite different Poisson–Boltzmann method (Delphi

Table 7. *The formal charges of metals and ionizable groups in different pH ranges*

		pH 4.6 |e|	pH 5.6–8.5 |e|	pH 10.6 |e|
Asp	OD1	−0.5	−0.5	−0.5
	OD2	−0.5	−0.5	−0.5
Glu	OE1	−0.25	−0.5	−0.5
	OE2	−0.25	−0.5	−0.5
Lys	NZ	1.0	1.0	0.5
Arg	NH1	0.5	0.5	0.5
	NH2	0.5	0.5	0.5
Cys	S	−1.0	−1.0	−1.0
Oxt		−1.0	−1.0	−1.0
Nxt[a]		0.0	0.0	0.0
Cd		2.0	2.0	2.0
Zn		2.0	2.0	2.0

[a]The Nxt values are set to zero, because N-terminals of these three MTs are acetylated.

program in InsightII). Salt concentration is parameterized as 0.0 M, because electrostatic potentials change little in experimental salt concentrations range. The internal and external dielectric constants are set to 1 and 80, respectively. Electrostatic potentials are computed by mapping the molecules in a 105 × 105 × 105 lattice, using as boundary conditions previously calculated potential values evaluated with a coarse grid resolution (focusing strategy). This procedure gives a final resolution of 0.5 Å per grid unit. The formal charges of metals and ionizable residues are listed in Table 7 (the pH ranges are taken from experimental circumstances).

Only pH 5.6–8.5 and pH 10.6 ranges are considered because calculations show that 1 Glu does not have obvious effects on the electrostatic potentials as 8 Lys do.

Supplementary material in the Electronic Appendix

Tables of the existence behaviors of rabbit MTs in different buffers, crystallization, and preliminary X-ray data of rabbit MT-11. The Cartesian coordinates of the monomers, dimers, trimers, and tetramers of rat MT-11, rabbit MT-1 and -II (ASCII files, PDB format). This material is available free of charge via the Internet at http://pubs.acs.org.

Acknowledgments

The first two authors contributed equally. This project is supported by NCSF 29992590-2 and 29573095 of the People's Republic of China.

References

An Y, Li GP, Ru BG. 1999. Crystallization and preliminary X-ray studies of metallothionein II from rabbit liver. *Acta Crystallogr D55*:1242–1243.

Andersen RA, Daae HL. 1998. Preparation of metallothionein from rat liver and studies of its properties with respect to use as a standard in gel permeation chromatography, polyacrylamide gel systems, autoradiography and Western blotting. *Comp Biochem Physiol B 90*:59–67.

Andersen RA, Daae HL, Mikalsen A, Alexander J. 1989. Occurrence of various forms of metallothionein in the rat after a short-term cadmium injection regimen. *Comp Biochem Physiol C93*:367–375.

Arthur JR, Bremner I, Morrice PC, Mils CF. 1987. Stimulation of peroxidation in rat liver microsomes by (copper, zinc)-metallothioneins. *Free Radic Res Commun 4*:15–20.

Chatterjee A, Maiti IB. 1987. Purification and immunological characterization of catfish (*Heteropneustes fossilis*) metallothionein. *Mol Cell Biochem 78*:55–64.

Gasull T, Rebollo DV, Romero B, Hidalg J. 1993. Development of a competitive double antibody radioimmunoassay for rat metallothionein. *J Immunoassay 14*:209–225.

Hidalgo J, Bernues J, Thomas DC, Garvey JS. 1998. Effect of 2-mercaptoethanol on the electrophoretic behavior of rat and dogfish metallothionein and chromatographic evidence of a naturally occurring metallothionein polymerization. *Comp Biochem Physiol C 89*:191–196.

Irons RD, Smith JC. 1976. Prevention by copper of cadmium sequestration by metallothionein in liver. *Chem Biol Interact 15*:289–294.

Kimura M, Koizumi S, Otsuka F. 1991. Detection of carboxymethylmetallothionein by sodium dodecyl sulfate-polyacrylamide gel electrophoresis. *Methods Enzymol 205*:114–119.

Kojima Y. 1991. Definition and nomenclature of metallothioneins. *Methods Enzymol 205*:8–10.

Lee B, Richards FM. 1971. The interpretation of protein structures: Estimation of static accessibility. *J Mol Biol 55*:379–400.

Melis KA, Carter DC, Stout CD, Winge DR. 1983. Single crystals of cadmium, zinc metallothionein. *J Biol Chem 258*:6255–6257.

Otsuka F, Koizumi S, Kimura M, Ohsawa M. 1988. Silver staining for carboxymethylated metallothioneins in polyacrylamide gels. *Anal Biochem 168*:184–192.

Palumaa P, Mackay EA, Vasak M. 1992. Nonoxidative cadmium-dependent dimerization of cadmium-metallothionein from rabbit liver. *Biochemistry 31*:2181–2186.

Palumaa P, Vaher M. 1996. Metal-induced dimerization of Cd_7-metallothionein role of anions. *Ann Clin Lab Sci 26*:264–268.

Palumaa P, Vasak M. 1992. Binding of inorganic phosphate to the cadmium-induced dimeric form of metallothionein from rabbit liver. *Eur J Biochem 205*:1131–1135.

Robbins AH, Mcree DE, Williamson M, Collett SA, Xuong NH, Furey WF, Wang BC, Stout CD. 1991. Refined crystal structure of Cd, Zn metallothionein at 2.0 Å resolution. *J Mol Biol 221*:1269–1293.

Robbins AH, Stout CD. 1991. X-ray structure of metallothionein. *Methods Enzymol 205*:485–502.

Tsai CJ, Lin SL, Wolfson HJ, Nussinov R. 1997. Studies of protein–protein interface: A statistical analysis of the hydrophobic effect. *Protein Sci 6*:53–61.

Vallee L. 1991. Introduction to metallothionein. *Methods Enzymol 205*:3–7.